Total cross-section and diffractive ρ^0 production in $\gamma\gamma$ collisions at LEP

Ákos Csilling[a*] on behalf of the L3 Collaboration

[a]KFKI Research Institute for Particle and Nuclear Physics
H-1525 Budapest, P.O.Box 49, Hungary

The reaction $e^+e^- \rightarrow e^+e^-\gamma^*\gamma^* \rightarrow e^+e^-$ *hadrons* is analysed for quasi-real virtual photons using data collected by the L3 detector during the LEP high energy runs at $\sqrt{s} = 183$ and 189 GeV. Preliminary results on the cross sections $\sigma(e^+e^- \rightarrow e^+e^-$ *hadrons*$)$ and $\sigma(\gamma\gamma \rightarrow$ *hadrons*$)$ are given in the interval 5 GeV $\leq W_{\gamma\gamma} \leq$ 145 GeV. The centre-of-mass energy dependence of the two-photon cross section is well described by the universal Regge parametrisation, but with a steeper rise with energy as compared to hadron-hadron cross sections. The data are also compared to the expectations of different theoretical models. To investigate diffractive processes, the elastic $\gamma\gamma \rightarrow \rho^0\rho^0$ process and the inclusive ρ^0 production $\gamma\gamma \rightarrow \rho^0 X$ are studied in the $W_{\gamma\gamma} \geq 3$ GeV region. In all channels a comparison is made with the Pythia and Phojet Monte Carlo generators.

1. INTRODUCTION

The $e^+e^-\rightarrow e^+e^-\gamma^*\gamma^*\rightarrow e^+e^-$*hadrons* process is a copious source of hadron production at high energies. The hadron system has predominantly a low mass value. A large fraction of the hadrons escape detection due to the large diffractive cross section and the Lorentz boost of the $\gamma\gamma$ system. For these events, the measured effective mass $W_{\rm vis}$ is smaller than the centre of mass energy of the two interacting photons $W_{\gamma\gamma}$. In this reaction most of the initial energy is taken by the scattered electrons and positrons. We analyse only data where these are not detected (anti-tagged events).

New results are presented on the total cross section $\sigma(e^+e^-\rightarrow e^+e^-$*hadrons*$)$ for the e^+e^- centre of mass energy of $\sqrt{s}$= 183 GeV and $\sqrt{s}$= 189 GeV. The two-photon cross section $\sigma(\gamma\gamma \rightarrow$ *hadrons*$)$ is then derived in the interval 5 $\leq W_{\gamma\gamma} \leq$ 145 GeV. The analysis of the data taken at $\sqrt{s}$= 130-161 GeV has been published [1].

*This work was partly supported by the Hungarian Scientific Research Fund OTKA under contract numbers F-023259 and T-019181. Participation at this conference was supported by the National Committee for Technological Development under contract number OMFB-00664/99/, and the conference organisers.

2. TOTAL CROSS-SECTION

2.1. Event selection

Data have been collected with the L3 detector [2,3] at $\sqrt{s}$= 182.72 GeV with a total integrated luminosity of 51.35 pb^{-1} during 1997 and at $\sqrt{s}$= 189 GeV with a total integrated luminosity of 171.8 pb^{-1} during 1998.

Hadronic two-photon events are selected by the following criteria :

- At least six particles must be detected. A particle can be a track, a photon or a pion cluster in the hadron calorimeter or in the luminosity monitor.
- The total energy in the electro-magnetic calorimeter is required to be greater than 500 MeV. The total energy deposited in the calorimeters must be below 40% of the collision energy.
- An anti-tag condition excludes events with an electromagnetic shower shape and energy greater than 70 GeV in the luminosity monitor, in a fiducial region of 33-64 mrad. The Q^2 value of the selected events is thus smaller than 8 GeV^2, in average $\langle Q^2\rangle \sim 1.5\ 10^{-2}$ GeV^2.

After selection, the background from beam-gas and beam-wall interactions is found to be negligible. The analysis is limited to events with $W_{\rm vis}\geq$ 5 GeV. More than 1 million events are selected.

The $\gamma\gamma \rightarrow$ *hadrons* processes are simulated

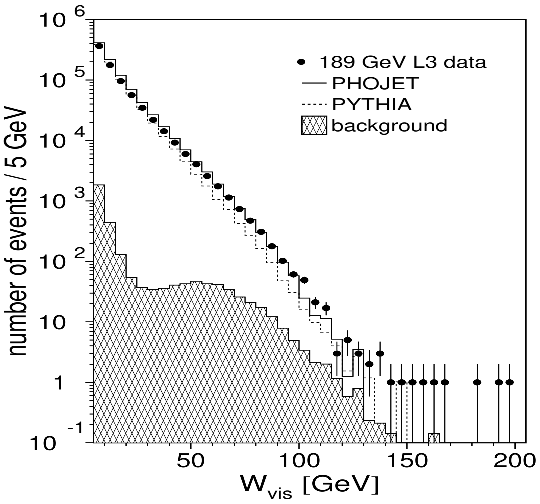

Figure 1. The measured hadronic mass W_{vis}. The backgrounds due to e^+e^-annihilation and $e^+e^- \to e^+e^-\tau\tau$ are indicated as a shaded area.

with the PHOJET[2] [4] and PYTHIA[3] [5] event generators. The background processes $e^+e^- \to$ *hadrons*(γ), $ZZ(\gamma)$, $Zee(\gamma)$, $We\nu(\gamma)$, $\tau^+\tau^-(\gamma)$, W^+W^- and $e^+e^-\tau^+\tau^-$ were simulated and subtracted. At low masses the background is below 1%, dominated by the two-photon τ production. It increases at high masses, due to annihilation processes, and reaches a maximum of 12% at 145 GeV. In Figure 1 the W_{vis} spectrum is shown for the $\sqrt{s}=$ 189 GeV data. The trigger efficiency is mass dependent, for the $\sqrt{s}=$ 189 GeV data it varies from 78% at W_{vis}=5 GeV to 94% for $W_{\mathrm{vis}}>$ 80 GeV.

2.2. Unfolding and efficiency

From the observed distribution of the visible effective mass, W_{vis}, the true hadron mass $W_{\gamma\gamma}$ distribution must be extracted. The number of observed events are then corrected for the efficiency and acceptance of the detector.

The measured W_{vis} spectrum is weakly correlated to the total centre of mass energy of the $\gamma\gamma$ system because part of the produced particles may go undetected in the forward and backward regions. In order to obtain the $W_{\gamma\gamma}$ distribution from the W_{vis} spectrum the method of [6] is used.

After unfolding the events are corrected for detector acceptance and efficiency. There is a systematic difference of $\simeq$ 20% between the results obtained with the two Monte Carlo models, which may be attributed to a different modelling of the diffractive interactions which are not easily seen in the detector.

2.3. Cross sections and systematic errors

From the number of events the cross section $d\sigma(\ e^+e^- \to e^+e^-$ *hadrons*$)$ is measured. To extract the total cross section of two real photons the photon flux $\mathcal{L}_{\gamma\gamma}$[7] is calculated using the method described in [8] and the hadronic two-photon cross-section is extrapolated to zero Q^2 using the form factors of [9]. Depending on the form factors used, this calculation may vary by $\pm$10% [8].

The systematic errors are evaluated for each $W_{\gamma\gamma}$ bin. The main sources are:

- uncertainties on the trigger are 5% at $W_{\gamma\gamma}=$ 5 GeV and 2% at $W_{\gamma\gamma}=$ 145 GeV.
- uncertainties on the energy scale of the calorimeters excluding the clusters measured in the luminosity calorimeter are $\simeq 1-2\%$.
- the cut on the number of particles gives a systematic error of 10% at $W_{\gamma\gamma}=$ 5 GeV and $\simeq$ 1% at $W_{\gamma\gamma}=$ 145 GeV.

The mass dependent statistical and systematic errors are added in quadrature in each $W_{\gamma\gamma}$ bin. The uncertainty related to the Monte Carlo model is not added to the systematic errors, but the complete analysis is done for PYTHIA as well as for PHOJET. The discrepancy on the cross section reflects the difference on selection efficiency given by the two generators. The $\gamma\gamma \to$ *hadrons* cross sections unfolded with PHOJET at $\sqrt{s}=$ 183 GeV and $\sqrt{s}=$ 189 GeV are compared in Figure 2. The data are compatible within systematic errors.

2.4. Regge parametrisation

Total hadronic cross sections show a characteristic steep decrease in the region of low centre of mass energy followed by a slow rise at high energies. A. Donnachie and P.V. Landshoff [10]

[2] PHOJET version1.05c
[3] PYTHIA version 5.718 and JETSET version 7.408

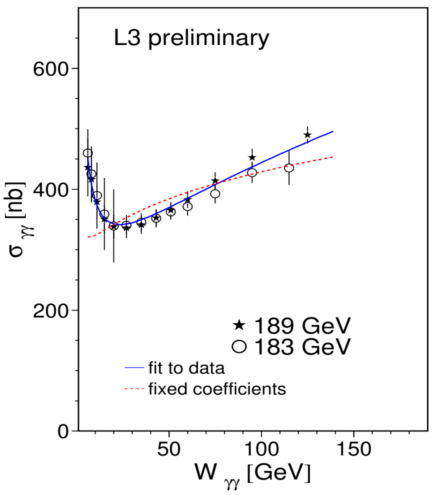

Figure 2. The data at $\sqrt{s}$= 189 GeV are compared to the data at $\sqrt{s}$= 183 GeV The Regge fits described in the text are superimposed to the data corrected with PHOJET.

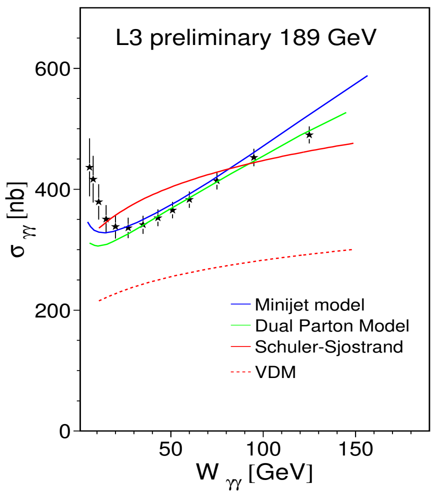

Figure 3. Comparison of the data with various models predictions (see text). The data are corrected with PHOJET. The errors are statistical and systematic added in quadrature.

showed that a parametrisation of the form

$$\sigma_{\rm tot} = A\, s^{\epsilon} + B\, s^{-\eta} \qquad (1)$$

can account for the energy behaviour of all total cross sections, the powers of s being universal. In a recent compilation of the total cross section data [11] a fit of Equation 1 for all hadron total cross sections gives a result compatible with the universal values of $\epsilon = 0.095 \pm 0.002$ and $\eta = 0.34 \pm 0.02$. The coefficients A and B are process and Q^2 dependent.

This expression may also be valid for the two-photon total hadronic cross section. The data are fitted to Equation 1 with the parameters ϵ and η fixed to the world average value. The coefficients A and B are highly correlated, the correlation being $\sim$ -0.8. The fit does not represent well the $\sigma_{\gamma\gamma}$ energy dependence, we therefore try a fit with A, B and ϵ as free parameters. The fits are shown in Figure 2 and the results given in Table 1. The obtained value $\epsilon = 0.222 \pm 0.019$ is more than a factor two higher than the universal value. In PDG 1996 [12] a different universal fit was given, but with these values the factor two difference is conserved, showing that the fitted value of ϵ is strongly correlated to η. We try to avoid this by fitting only the Pomeron exchange for sufficiently high $W_{\gamma\gamma}$ values. The results, using different minimum values of $W_{\gamma\gamma}$ and different Monte Carlo generators for unfolding are listed in Table 1. We observe also that the value of ϵ increases by increasing the lower mass cutoff, thus indicating a somewhat variable slope due to the onset of QCD phenomena.

2.5. Models for $\gamma\gamma$ total cross sections

Three models describing the total $\gamma\gamma$ cross section are compared to our data in Figure 3.

The model of G.A. Schuler and T. Sjöstrand [13] aims at a smooth superposition of hadron-like and point-like photon interactions. Following their discussion, one sees that the fluctuation of both photons into vector mesons is not sufficient to describe the data. Adding the point-like splitting of the photon to $q\bar{q}$ pairs, the cross section increases to values comparable to our data points.

The cross sections predicted by R. Engel and J. Ranft [4] are in good agreement with the data.

fit	$W_{\gamma\gamma}$ interval	A	B	η fixed	ϵ	C.L.
PDG98 (PHOJET)	5-145 GeV	50.±9.	1153.±114.	0.34	0.222±0.019	0.995
PDG98 (PHOJET)	5-145 GeV	172.±3.	325.±65.	0.34	0.095 fixed	0.000034
PDG96 (PHOJET)	5-145 GeV	90.±10.	1519.±169.	0.468	0.168±0.012	0.895
PDG98 (PYTHIA)	5-145 GeV	78.±10.	753.±116.	0.34	0.206±0.013	0.61
(PHOJET)	13-145 GeV	230±10	—	—	0.070±0.006	$< 10^{-6}$
(PHOJET)	31-145 GeV	150±8	—	—	0.118±0.007	0.06
(PHOJET)	39-145 GeV	126±8	—	—	0.136±0.008	0.45
(PHOJET)	47-145 GeV	115±9	—	—	0.146±0.010	0.46
(PYTHIA)	13-145 GeV	185±7	—	—	0.118±0.005	$< 10^{-6}$
(PYTHIA)	31-145 GeV	145±6	—	—	0.146±0.006	0.05
(PYTHIA)	39-145 GeV	135±7	—	—	0.153±0.006	0.04
(PYTHIA)	47-145 GeV	131±9	—	—	0.156±0.010	0.14

Table 1
Fit to the total cross section of the form [10] $\sigma_{\gamma\gamma}= A\, s^{\epsilon} + B\, s^{-\eta}$, where $s = W^2_{\gamma\gamma}$. The statistical and experimental errors and the correlation matrix between the data points (in total 13 points at $\sqrt{s}$=183 GeV and 13 points at $\sqrt{s}$=189 GeV) are used in the fit. The fitted parameters are strongly correlated. The second set of fits evaluates only the increase of $\sigma_{\gamma\gamma}$ with s, i.e. the Pomeron part of the fit. PHOJET and PYTHIA in the first column indicate the Monte Carlo used in unfolding the data.

In their model γp and pp data are used to fix the couplings of the Pomeron and of the Reggeon to the $q\bar{q}$ fluctuation of the photon. The cross sections are then calculated in the framework of a Dual Parton Model, with the unitarization constraint [4].

The calculation of the mini-jet model of R.M. Godbole and G. Pancheri [14] ascribes to QCD the task of calculating the average number of semi-hard collisions $n(b, s)$, which is a function of the impact parameter b and of the centre of mass energy s. The collisions are assumed to be independent of each other at a fixed value of the impact parameter b and to have a Poisson type distribution around the average value. In Figure 3 the parameters which fit best the photoproduction data are used ($p_{T\min} = 2$ GeV and $k_0 = 0.66$ GeV), together with the GRV parton density function.

3. EXCLUSIVE ρ^0 PAIR PRODUCTION

Since photons can fluctuate directly into neutral Vector Mesons, the $\gamma\gamma \to \rho^0\rho^0$ cross-section is expected to remain large at high $\gamma\gamma$ centre-of-mass energies [15] ("elastic" $\gamma\gamma$ scattering). A measurement performed at large $W_{\gamma\gamma}$, above the well known but still controversial $\rho^0\rho^0$ threshold enhancement [16], can help to understand the behaviour of quasi-elastic and diffractive processes.

The exclusive $e^+e^- \to e^+e^-\pi^+\pi^-\pi^+\pi^-$ events are selected by requiring four tracks, with a distance of closest approach to the nominal vertex smaller than 1 mm in the transverse plane, total charge equal to zero and missing transverse momentum squared smaller than 0.05 GeV^2. In the $\sqrt{s}$= 189 GeV sample, we have selected 14000 events. The 4π mass spectrum is dominated by the low mass threshold enhancement and agrees well with previous measurements [16].

There are 843 events with a mass $W_{\gamma\gamma}$> 3 GeV. The four tracks in each event give rise to four possible $\pi^+\pi^-$ neutral combinations. The equal charge $\pi^+\pi^+$ and $\pi^-\pi^-$ combinations are used to subtract the combinatorial background. Figure 4 shows the $\pi^+\pi^-$ mass distribution after subtraction of the equal charge combinations. A peak in the ρ^0 mass range is visible, a Breit-Wigner fit

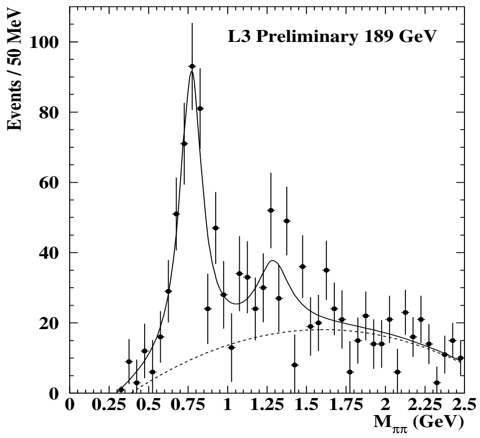

Figure 4. Effective mass of two opposite-charge pions, after subtraction of background estimated from equal-charge combinations.

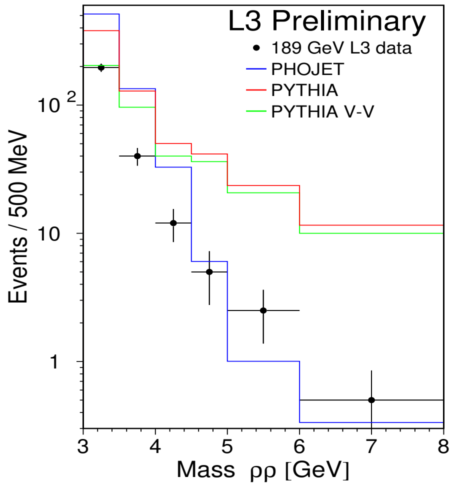

Figure 5. Number of $\rho\rho$ events as a function of $W_{\gamma\gamma}$. The data are compared to Monte Carlo predictions.

gives $M_\rho = 768 \pm 7$ MeV, $\Gamma_\rho = 170 \pm 20$ MeV. A second enhancement is also visible between 1.2 and 1.4 GeV, which corresponds to the f_2 resonance, the Breit-Wigner fit gives $M_{f_2} = 1288 \pm 22$ MeV, $\Gamma_{f_2} = 258 \pm 135$ MeV. Since the f_2 cannot be produced diffractively, this indicates the presence of non-diffractive processes. A $\rho^0\rho^0$ region is defined by requiring both simultaneous $\pi^+\pi^-$ combinations to have masses below 1.2 GeV. The $W_{\gamma\gamma}$ distribution of the $\rho^0\rho^0$ events is shown in Figure 5. Exclusive $\gamma\gamma\rightarrow$ VV events were generated with the PYTHIA Monte Carlo, the dominant channel being $\gamma\gamma\rightarrow\rho^0\rho^0$. PYTHIA expects too many events at high masses, while the mass-dependence of PHOJET is too steep.

4. INCLUSIVE ρ^0 PRODUCTION

We study single diffractive dissociation in the inclusive process $\gamma\gamma \rightarrow \rho^0 X$ with $\rho^0 \rightarrow \pi^+\pi^-$ using data collected at $\sqrt{s} = 183$ GeV, corresponding to $\mathcal{L} = 47.9$ pb^{-1}. This process yields a larger number of events compared to the exclusive $\rho^0\rho^0$ production at the price of higher background. Higher invariant masses are accessible, but events can not be fully reconstructed.

We select events with $W_{\rm vis} > 2$ GeV and ρ^0 candidates with $p_T > 1$ GeV and $|\cos\vartheta| < 0.8$ in the laboratory. Within this kinematic region the detection efficiency is uniform.

Diffractive events in general contain a rapidity gap that separates the final state particles originating from the two incoming photons. In order to separate non-diffractive production, we require the ρ^0 candidate to have the largest or smallest rapidity in the event, excluding its decay products.

Background is subtracted in two steps. First all combinations of two equal-charge tracks are treated as candidates, subject to the same cuts, and subtracted from the mass distribution of real candidates with opposite-charged tracks. The resulting mass distribution is fitted with a Breit-Wigner curve with fixed parameters $M = 770$ MeV and $\Gamma = 150$ MeV and a background of the form $e^{A(x-280\text{ MeV})}(1 - e^{B(x-280\text{ MeV})})$.

The number of events observed after background subtraction is shown in Table 2, together with the numbers expected from three Monte

	$W_{\gamma\gamma}$ cut	$W_{\rm vis} > 2$ GeV	$W_{\rm vis} > 3$ GeV	$W_{\rm vis} > 5$ GeV
Data		202.4 ± 40.0	77.1 ± 23.9	34.3 ± 6.8
PYTHIA	3.0 GeV	123.7 ± 15.6	108.7 ± 12.5	74.3 ± 8.0
PYTHIA VV	2.5 GeV	98.6 ± 7.6	82.6 ± 6.8	35.6 ± 2.3
PHOJET	3.0 GeV	12.9 ± 10.9	6.2 ± 5.9	—

Table 2
Number of inclusive $\gamma\gamma \to \rho^0 X$ events after background subtraction.

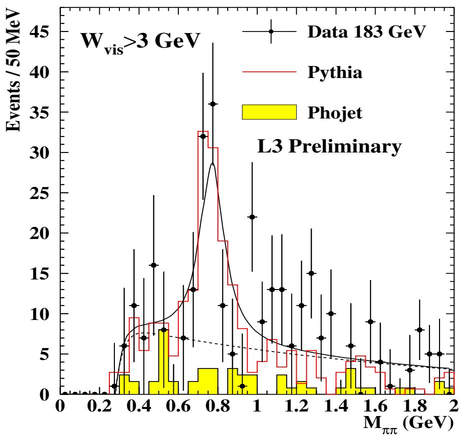

Figure 6. Mass distribution of two opposite-charged pions after subtraction of background estimate from two equal-charged pions. The data are compared to Monte Carlo predictions and fitted as signal plus background.

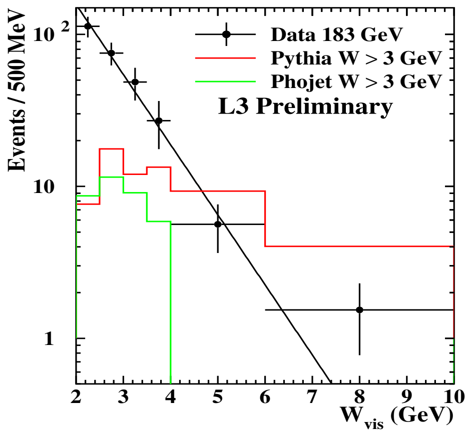

Figure 7. Number of $\gamma\gamma \to \rho^0 X$ events as a function of $W_{\rm vis}$. The data are compared to the PYTHIA and PHOJET Monte Carlo predictions.

Carlo samples: full PYTHIA $\gamma\gamma \to$ *hadrons*, PYTHIA containing only diffractive $\gamma\gamma \to VV$, with $V = \rho^0, \omega^0, \phi$, and full PHOJET $\gamma\gamma \to$ *hadrons*. The lower value of the generated $W_{\gamma\gamma}$ is also given in the table.

Figure 6 shows the mass distribution of the ρ^0 candidates for $W_{\rm vis} > 3$ GeV. The strong ρ^0 signal is well reproduced by PYTHIA, while it is absent in PHOJET.

To test the diffractive nature of our sample, the decay angle of the ρ^0 candidates is studied. Conservation of the s-channel helicity implies transverse polarization for diffractive ρ^0 production from $Q^2 = 0$ photons, while non-diffractive ρ^0 production is unpolarized. We define ϑ^* as the angle between the π^+ momentum in the ρ^0 frame and the ρ^0 momentum in the $\gamma\gamma$ rest frame as measured by the visible hadronic system. This angle is not the true decay angle, but Monte Carlo simulations show that the $\cos\vartheta^*$ resolution is $\sigma_{\cos\vartheta^*} = 0.033$. A fit of $\sin^2\vartheta^*$, corresponding to purely transverse polarization, gives $\chi^2 = 1.82$ (77% CL), while a fit with a constant, corresponding to unpolarized decay, gives $\chi^2 = 6.18$ and a confidence level of 19%.

Figure 7 shows the number of events observed after background subtraction as a function of $W_{\rm vis}$, together with predictions from PYTHIA and

PHOJET. Note that both Monte Carlo samples have a generator level cut at $W_{\gamma\gamma} > 3$ GeV, so in the first two bins they are expected to be low. PHOJET predicts too few events, while the PYTHIA distribution is too flat.

The p_T^2 distribution after correction for detector effects using the sample of vector meson pairs generated by PYTHIA was fitted between 1 GeV$^2 \leq p_T^2 < 3$ GeV^2 by an exponential function, and the preliminary slope parameter is -2.04 ± 0.11 GeV^{-2}.

5. CONCLUSIONS

The cross section $\sigma(\mathrm{e^+e^-} \rightarrow \mathrm{e^+e^-}\,hadrons)$ for untagged events is measured at LEP, with the L3 detector, at $\sqrt{s} = 183$ and 189 GeV, in the interval 5 GeV$\leq W_{\gamma\gamma} \leq$ 145 GeV. The real photon total cross section $\sigma(\gamma\gamma \rightarrow hadrons)$, derived from the data, increases as a function of $W_{\gamma\gamma}$, faster than expected from the universal fit of hadron-hadron total cross-sections. The observed energy dependence can be reproduced by QCD models which include hard scattering of the partons inside the photon.

An analysis of $\gamma\gamma \rightarrow \rho^0\rho^0$ and $\gamma\gamma \rightarrow \rho^0 X$ events has been performed. In the region 3 GeV$\leq W_{\gamma\gamma} \leq$ 10 GeV both PYTHIA and PHOJET fail to reproduce the data : the energy dependence of $\rho^0\rho^0$ production is too flat in PYTHIA and too steep in PHOJET. In the $\gamma\gamma \rightarrow \rho^0 X$ sample the ρ^0 is transversely polarised as expected by s-channel helicity conservation. Almost no ρ^0 is produced by PHOJET in the studied kinematical region.

ACKNOWLEDGEMENTS

I would like to express my gratitude to Maria N. Kienzle-Focacci and Evelyne Delmeire for providing their results and for useful discussions and encouragement.

REFERENCES

1. L3 Coll., M. Acciari et al.,Phys. Lett. **B 408** (1997) 450.
2. L3 Coll., B. Adeva et al., Nucl. Inst. Meth. **A 289** (1990) 35.
3. M. Acciarri et al., Nucl. Inst. Meth. **A 351** (1994) 300.
4. R. Engel, Z. Phys. **C 66** (1995) 203 ;
   R. Engel and J. Ranft, Phys. Rev. **D 54** (1996) 4246;
   and R. Engel private communication.
5. T. Sjöstrand, Comput. Phys. Commun. **82** (1994) 74.
6. G. D'Agostini, Nucl. Inst. Meth. **A 362** (1995) 487.
7. V.M. Budnev, I.F. Ginzburg, G.V. Meledin and V.G. Serbo, Phys. Rep. **C 15** (1974) 181.
8. G.A. Schuler, Improving the equivalent-photon approximation in electron-positron collisions, hep-ph/9610406, CERN-TH/96-297.
   We wish to thank the author for providing us with the numerical integration program of the luminosity function.
9. J.J. Sakurai and D. Schildknecht, Phys. Lett. **B 40** (1972) 121.
10. A. Donnachie and P.V. Landshoff, Phys. Lett. **B 296** (1992) 227.
11. Review of Particle Physics, Eur. Phys. J. **C 3** (1998) 1.
12. Review of Particle Physics, Phys. Rev. **D 54** (1996) 1.
13. G.A. Schuler and T. Sjöstrand, Nucl. Phys. **B 407** (1993) 539 ;
    G.A. Schuler and T. Sjöstrand, Z. Phys. **C 73** (1997) 677.
14. R.M. Godbole and G. Pancheri, hep-ph/9903331 (1999);
    A. Corsetti, R.M. Godbole and G. Pancheri, Phys. Lett. **B 435** (1998) 441.
15. V.L. Chernyak and I.R. Zhitnitsky, Nucl. Phys. **B 222** (1983) 382.
16. ARGUS Coll., H. Albrecht *et al.*, Z. Phys. **C 50** (1991) 1;
    PLUTO Coll., Berger *et al.*, Z. Phys. **C 38** (1988) 521;
    TPC/2γ Coll., Aihara et al., Phys. Rev. **D 37** (1988) 28.